Author/s:
Xu, B;Anderson, BM;Mountford, SJ;Thompson, PE;Mintern, JD;Edgington-Mitchell, LE

Title:
Cathepsin X deficiency alters the processing and localisation of cathepsin L and impairs cleavage of a nuclear cathepsin L substrate

Date:
2024-05-01

Citation:
Xu, B., Anderson, B. M., Mountford, S. J., Thompson, P. E., Mintern, J. D. & Edgington-Mitchell, L. E. (2024). Cathepsin X deficiency alters the processing and localisation of cathepsin L and impairs cleavage of a nuclear cathepsin L substrate. Biological Chemistry, 405 (5), pp.351-365. https://doi.org/10.1515/hsz-2023-0355.

Persistent Link:
https://hdl.handle.net/11343/345482

Bangyan Xu, Bethany M. Anderson, Simon J. Mountford, Philip E. Thompson, Justine D. Mintern and Laura E. Edgington-Mitchell*

Cathepsin X deficiency alters the processing and localisation of cathepsin L and impairs cleavage of a nuclear cathepsin L substrate

https://doi.org/10.1515/hsz-2023-0355
Received November 29, 2023; accepted February 12, 2024;
published online February 28, 2024

Abstract: Proteases function within sophisticated networks. Altering the activity of one protease can have sweeping effects on other proteases, leading to changes in their activity, structure, specificity, localisation, stability, and expression. Using a suite of chemical tools, we investigated the impact of cathepsin X, a lysosomal cysteine protease, on the activity and expression of other cysteine proteases and their inhibitors in dendritic cells. Among all proteases examined, cathepsin X gene deletion specifically altered cathepsin L levels; pro-cathepsin L and its single chain accumulated while the two-chain form was unchanged. This effect was recapitulated by chemical inhibition of cathepsin X, suggesting a dependence on its catalytic activity. We demonstrated that accumulation of pro- and single chain cathepsin L was not due to a lack of direct cleavage by cathepsin X or altered glycosylation, secretion, or mRNA expression but may result from changes in lysosomal oxidative stress or pH. In the absence of active cathepsin X, nuclear cathepsin L and cleavage of the known nuclear cathepsin L substrate, Lamin B1, were diminished. Thus, cathepsin X activity selectively regulates cathepsin L, which has the potential to impact the degree of cathepsin L proteolysis, the nature of substrates that it cleaves, and the location of cleavage.

Keywords: activity-based probes; cathepsins; cysteine proteases; dendritic cells; nuclear proteolysis; protease networks

***Corresponding author: Laura E. Edgington-Mitchell**, Department of Biochemistry & Pharmacology, Bio21 Molecular Science and Biotechnology Institute, The University of Melbourne, Parkville, VIC 3052, Australia, E-mail: laura.edgingtonmitchell@unimelb.edu.au

Bangyan Xu, Bethany M. Anderson and Justine D. Mintern, Department of Biochemistry & Pharmacology, Bio21 Molecular Science and Biotechnology Institute, The University of Melbourne, Parkville, VIC 3052, Australia

Simon J. Mountford and Philip E. Thompson, Medicinal Chemistry, Monash Institute of Pharmaceutical Sciences, Monash University, Parkville, VIC 3052, Australia

1 Introduction

Proteases are hydrolytic enzymes that cleave the peptide bonds of protein substrates and are responsible for protein degradation and turnover. Proteases contribute to diverse biological processes, including antigen processing, cell signalling, migration, maturation, and proliferation (Chapman et al. 1997; Hsing and Rudensky 2005; Jevnikar et al. 2008; Obermajer et al. 2008). Aberrant proteolytic activity is linked to various diseases, including cancer, inflammation, and cardiovascular diseases (Allan et al. 2017; Hua and Nair 2015; López-Otín and Bond 2008; Mitrovic et al. 2017). Cathepsins are a unique family of proteases that can be classified into three groups based on their mechanism of action, including cysteine, serine, and aspartic cathepsins. The cysteine cathepsin family is the most abundant family with 11 members, including cathepsin B, C, F, H, K, L, O, S, V, X and W (Turk et al. 2012).

Cysteine cathepsins are synthesised as inactive zymogens, and their activation requires proteolytic removal of propeptide(s). Most endopeptidases autoactivate, including cathepsin B, H, L, S, K, V and F (Mach et al. 1994; Ménard et al. 1998; McQueney et al. 1997; Somoza et al. 2000; Vasiljeva et al. 2003, 2005; Wang et al. 1998). The exopeptidases cathepsin C and cathepsin X require the activity of other proteases for activation. Pro-cathepsin C is cleaved by cathepsin L and S (Dahl et al. 2001). The catalytic cysteine of cathepsin X forms a disulphide linkage with a cysteine residue in its pro-domain, making its pro-form incapable of autoactivation. *In vitro*, cathepsin X is activated upon removal of the pro-domain by cathepsin L (Nägler et al. 1999).

Upon removal of the pro-domains, single chain cathepsins are proteolytically activated. Some cathepsins, including B, D, C, H and L, also undergo additional processing into a two-chain form, which is dependent on the cysteine protease legumain (Anderson et al. 2020; Edgington-Mitchell et al. 2015, 2016; Hamon et al. 2016; Maehr et al. 2005; Martínez-Fábregas et al. 2018; Shirahama-Noda et al. 2003). Upon cleavage, the heavy and light chains remain associated by disulfide bonds and catalytic activity is maintained (Figure 1A).

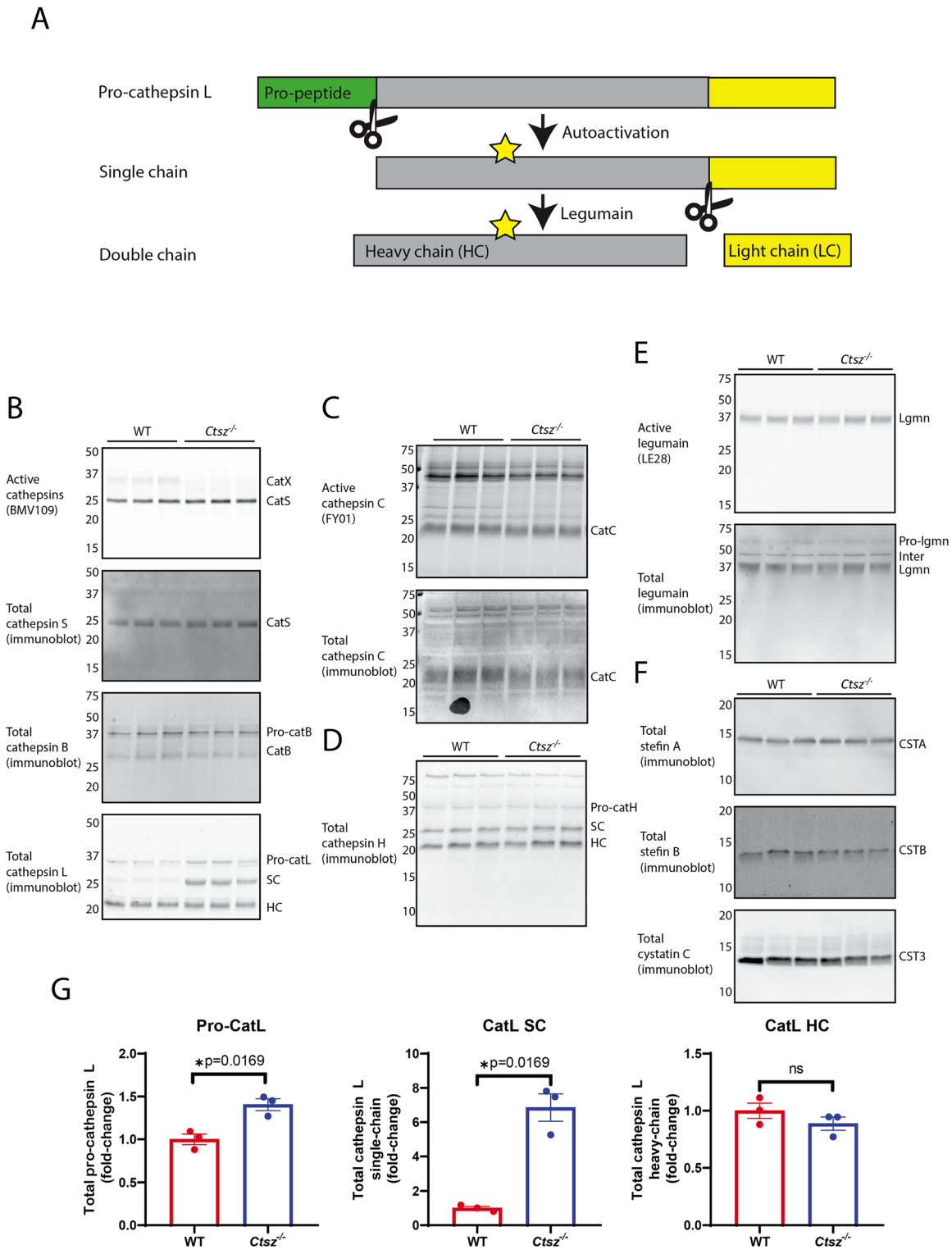

Figure 1: Analysis of lysosomal proteases and their inhibitors in the context of cathepsin X deficiency. (A) Schematic showing the post-translational processing of cathepsin L. (B) Live-cell labelling of WT (*hBIM*) and *Ctsz*$^{-/-}$ Mutu DCs with BMV109, as shown by in-gel fluorescence. Cathepsin B, S, and L immunoblots of WT (*hBIM*) and *Ctsz*$^{-/-}$ Mutu DCs. (C) Live-cell labelling of WT (*hBIM*) and *Ctsz*$^{-/-}$ Mutu DCs with FY01, as shown by in-gel fluorescence. Cathepsin C immunoblot of WT (*hBIM*) and *Ctsz*$^{-/-}$ Mutu DCs. (D) Cathepsin H immunoblot of WT (*hBIM*) and *Ctsz*$^{-/-}$ Mutu DCs. (E) Live-cell labelling of WT (*hBIM*) and *Ctsz*$^{-/-}$ Mutu DCs with LE28, as shown by in-gel fluorescence. Legumain immunoblot of WT (*hBIM*) and *Ctsz*$^{-/-}$ Mutu DCs. (F) Stefin A, B and Cystatin C immunoblot of WT (*hBIM*) and *Ctsz*$^{-/-}$ Mutu DCs. (G) Densitometry of 35, 27, and 23 kDa bands detected by cathepsin L immunoblot, displayed as average intensity for all WT (*hBIM*) and *Ctsz*$^{-/-}$ cells. Statistics were performed using unpaired Student's *t*-tests. Three technical replicates of bulk-sorted cells are shown, representative of >3 separate experiments. Error bars represent SEM. ns $p > 0.05$, *$p \leq 0.05$, **$p \leq 0.01$, ***$p \leq 0.001$, **** $p \leq 0.0001$.

Cathepsin X (also known as Z or P; gene name CTSZ) is a unique papain-like cysteine protease that mainly resides in the lysosomes of phagocytic cells, including monocytes, macrophages and dendritic cells (Kos et al. 2005). Cathepsin X shares only 26–35 % of overall homology with other cysteine cathepsins and has a comparatively short propeptide sequence (Deussing et al. 2000). Active cathepsin X is a monocarboxy-exopeptidase that cleaves one amino acid from the C terminus of its substrates with a pH optimum of 5.0 (Nägler et al. 1999). A number of studies have observed potential redundancies between cathepsin X and cathepsin B, whereby the expression of one is altered in the absence of the other (Bernhardt et al. 2010; Schwenck et al. 2019; Sevenich et al. 2010; Tamhane et al. 2014; Vasiljeva et al. 2006). Independent of its proteolytic activity, the propeptide of cathepsin X contains an RGD motif that can interact with αVβ3 integrin receptors to trigger downstream signalling events (Akkari et al. 2014; Campden et al. 2022).

To explore the influence of cathepsin X on the lysosomal protease network, we analysed the expression and processing of lysosomal proteases and their inhibitors in the context of cathepsin X deficiency. Loss of cathepsin X led to altered levels of cathepsin L, where its pro-form and single chain accumulated in cells lacking active cathepsin X. While the mechanism of this remains to be elucidated, a consequence is that less cathepsin L is trafficked to the nucleus in the absence of cathepsin X activity, resulting in impaired processing of its nuclear substrates.

2 Results

2.1 Cathepsin L processing is altered in cathepsin X-deficient cells

To investigate the impact of cathepsin X deficiency on the lysosomal protease network, we used immortalised murine dendritic cells, Mutu DCs, as a model system. These cells express various cysteine cathepsins, including X. We generated cathepsin X-deficient cells using CRISPR-Cas9 gene editing (Supplementary Figure S1A). Control cells were transduced with a vector containing Bcl-2-like 11 (*hBIM*)-specific guide RNA, which does not target the murine genome. Knockout efficiency was assessed by analysing cathepsin X activity with the activity-based probe (ABP) sCy5-Nle-SY and immunoblotting with a cathepsin X-specific antibody. Compared to *hBIM* control cells, the *Ctsz*-targeted cells exhibited a significant loss of cathepsin X activity and expression, while cathepsin S activity was unchanged (Supplementary Figure S1B).

We examined the expression and activity of select proteases and their endogenous inhibitors in wild-type and $Ctsz^{-/-}$ Mutu DCs. Using the pan-cysteine cathepsin probe BMV109, we first measured the activity of cathepsin B, L, S and X (Edgington-Mitchell et al. 2017; Verdoes et al. 2013). Labelling of cathepsin B and L was minimal compared to cathepsin S and X. Cathepsin S activity was not impacted by the loss of cathepsin X (Figure 1B). By immunoblot, cathepsin X-deficient cells showed no apparent changes in total expression and processing of cathepsin B and S (Figure 1B). The processing of cathepsin L, however, was altered: single-chain cathepsin L and, to a much lesser extent, pro-cathepsin L accumulated in the absence of cathepsin X (6.855-fold, $p = 0.0169$ and 1.405-fold, $p = 0.0112$, respectively) (Figure 1B and G). From the bulk-sorted cathepsin X-deficient cells, we generated single-cell clones (Supplementary Table 1, Supplementary Figure S2A and B). In all clones exhibiting complete loss of cathepsin X protein, cathepsin L single chain was increased compared to wildtype. In clones #4–6, where cathepsin X knockout was incomplete, cathepsin L was present mostly in its two-chain form. (Supplementary Figure S2A and B). Clone #6 exhibited some single chain accumulation but the fraction of total cathepsin L was lower than in the complete knockouts, suggesting potential concentration-dependent effects.

Using the cathepsin C activity-based probe, FY01 (Yuan et al. 2006), we did not observe any differences in cathepsin C activity (23 kDa; Figure 1C). Total expression and processing of cathepsin C by immunoblot were also unchanged (Figure 1C). Cathepsin H, which exhibits a similar processing mechanism as cathepsin L, was unchanged in the context of cathepsin X deficiency (Figure 1D).

As legumain is known to mediate the processing of the cathepsin L single chain, we hypothesised that single chain accumulation in the absence of cathepsin X might be mediated by altered legumain activity. However, using LE28, a legumain-specific activity-based probe (Edgington et al. 2013), and immunoblotting, we did not observe significant differences in total and active legumain between wild-type and $Ctsz^{-/-}$ cells (Figure 1E). Moreover, we did not observe changes in the expression of cysteine protease inhibitors, including stefin A, stefin B and cystatin C (Figure 1F).

Collectively, these results suggest that cathepsin X selectively regulates the single chain processing of cathepsin L in a legumain-independent manner.

2.2 Loss of cathepsin X activity drives accumulation of cathepsin L pro-form and single chain

To confirm whether loss of cathepsin X activity or its integrin-binding capabilities were responsible for inducing cathepsin L single chain accumulation, we attempted to rescue the phenotype of the cathepsin X-deficient cells with either wild-type, catalytically dead (R94S) or RGD mutant (R40H) cathepsin X constructs. Re-expression was assessed using the cathepsin X activity-based probe sCy5-Nle-SY and immunoblot (Mountford et al. 2020). WT (rWT) and R40H (rR40H) constructs recovered cathepsin X activity while rC94S was inactive, as expected (Figure 2A). The three cell lines all expressed similar levels of cathepsin X (Figure 2A).

By immunoblot, cells expressing inactive cathepsin X showed an accumulation of cathepsin L single chain, mirroring cathepsin X-deficient cells. In contrast, cathepsin L in the two cell lines expressing active cathepsin X was mostly present in the two-chain form, as observed in wild-type cells (Figure 2A and B). These results suggest that cathepsin L single chain accumulation depends on cathepsin X activity and not its RGD motif.

To pharmacologically modulate cathepsin X activity, we used Biotin-Hex-Nle-SY, an analogue of the activity-based probe sCy5-Nle-SY in which the Cy5 fluorophore was replaced with biotin. This molecule inhibited cathepsin X in both Mutu DCs and RAW264.7 cell lines, as shown by sCy5-Nle-SY labelling (Figure 2C and D). In Mutu DCs, cathepsin X inhibition and its gene deletion provoked an increase in both pro-cathepsin L (1.276-fold, p = 0.0333 and 1.572-fold, p = 0.0035, respectively) and its single chain (2.974-fold, p = 0.0040 and 3.779-fold, p = 0.0006, respectively) (Figure 2C and E). In RAW264.7 macrophages, cathepsin L single chain accumulated after cathepsin X inhibition (2.346-fold, p = 0.0047), while the pro-form and heavy chain were unchanged (Figure 2D and F).

Collectively, loss of cathepsin X activity leads to altered processing of cathepsin L. This phenomenon was not restricted to DCs but was also observed in macrophages. Accumulation of pro-cathepsin L was only observed in Mutu DCs.

2.3 Cathepsin L single chain does not accumulate due to a lack of direct processing by cathepsin X or changes in glycosylation or secretion, but may be influenced by oxidative stress or pH

Cathepsin X is a carboxy-exopeptidase that is not known to possess endopeptidase activity. While cathepsin L processing depends on the presence of active cathepsin X, we hypothesised that the effect was not likely to be through *direct* cleavage of cathepsin L by cathepsin X. To exclude this possibility, we incubated recombinant pro-cathepsin X with cathepsin L single chain *in vitro*. In an acidic buffer containing DTT, pro-cathepsin X is catalytically active, as demonstrated by labelling with the BMV109 ABP (Figure 3A). As reported previously (Nägler et al. 1999), cathepsin L cleaved pro-cathepsin X to form the mature 35 kDa form, which increased its activity (Figure 3A and B). Conversely, cathepsin L was not processed by either form of cathepsin X, as shown by immunoblotting (Figure 3C) or Coomassie stain (Figure 3D).

In further support of the hypothesis that cathepsin X does not *directly* process cathepsin L, cathepsin L heavy chain levels were unchanged in cathepsin X-deficient or inhibited cells (Figure 2C and E). If the single chain accumulated due to a lack of processing, the heavy chain should concomitantly decrease. Instead, cathepsin X-deficient cells exhibit increased total levels of intracellular cathepsin L compared to WT cells. It has recently been shown that loss of proteolytic activity of even one lysosomal protease (e.g., legumain) can provoke oxidative stress and activation of STAT3-dependent upregulation of other lysosomal proteases (Martínez-Fábregas et al. 2018; Wang et al. 2022). Using quantitative PCR, however, we showed that loss of cathepsin X did not promote transcription of cathepsin L mRNA (Figure 3E). In addition, lysosomal oxidative stress was not increased in cathepsin X-deficient cells (Figure 3F). By contrast, oxidative stress was significantly reduced (0.92-fold, p = 0.0022), suggesting that cathepsin X may promote oxidation. Endolysosomal pH was also increased in the absence of cathepsin X, as indicated by reduced pHrodo red fluorescence (0.83-fold, p = 0.0001) (Figure 3G).

We next questioned whether the multiple forms of cathepsin L were not the result of proteolytic processing, but instead due to differential glycosylation. To address this possibility, we treated WT and *Ctsz*$^{-/-}$ cell lysates with the glycosidase PNGase F. All three forms of cathepsin L exhibited greater gel mobility in response to deglycosylation, but there were no differences between WT and *Ctsz*$^{-/-}$ cells (Figure 3H).

We next investigated the hypothesis that cathepsin X deficiency leads to impaired secretion of the cathepsin L single chain, which would account for its intracellular accumulation. In wild-type cells, cathepsin L was primarily secreted in its pro-form and, to a lesser extent, in the two-chain form (Figure 3I and J). *Ctsz*$^{-/-}$ cells secreted significantly more pro-cat L and single-chain cathepsin L, while the heavy chain was unchanged. These results suggest

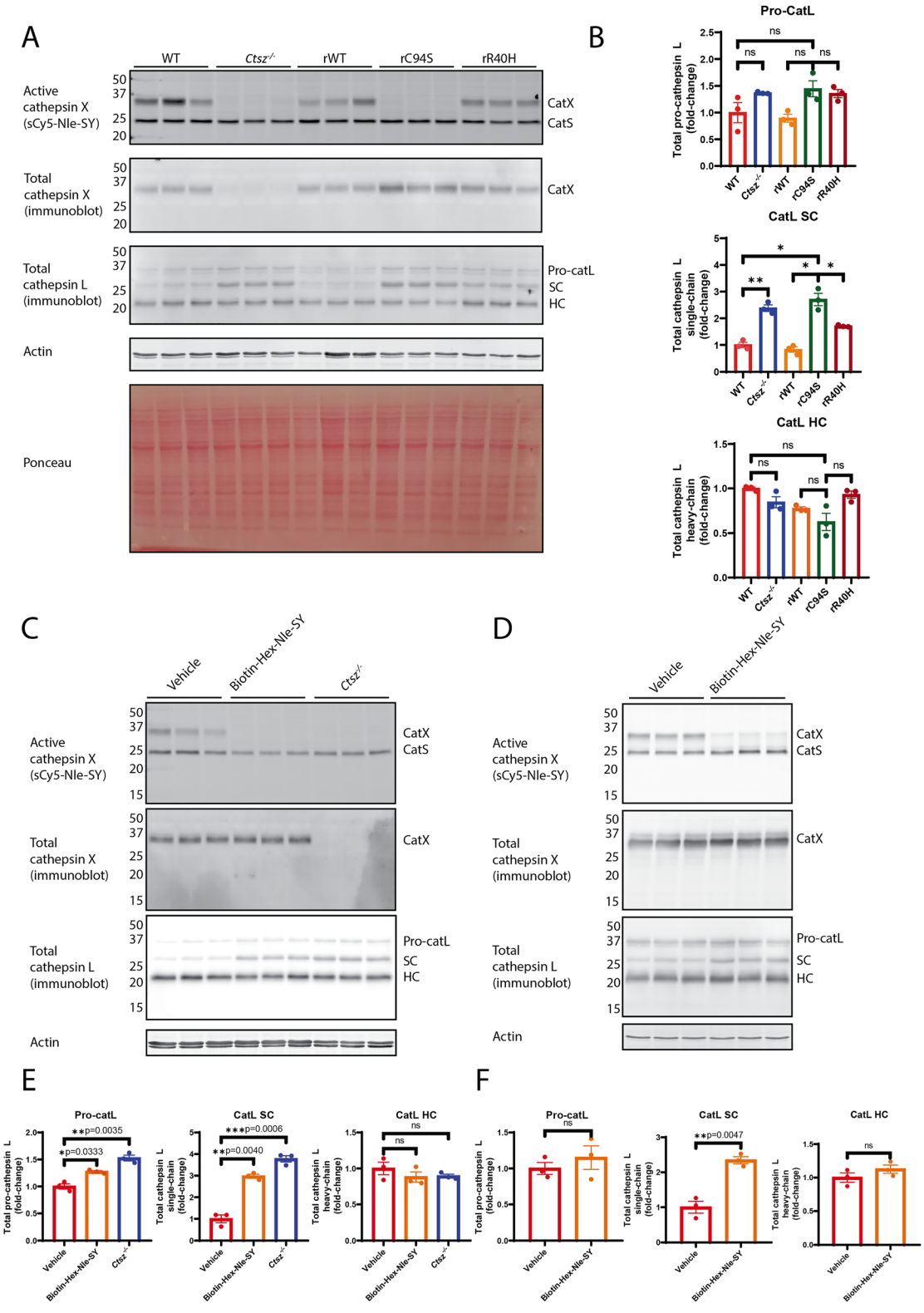

Figure 2: Processing of cathepsin L is influenced by active cathepsin X. (A) Live-cell labelling of Mutu DCs with sCy5-Nle-SY (WT (*hBIM*), *Ctsz*$^{-/-}$, *Ctsz*$^{-/-}$ re-expressing WT, C94S, and R40H), as shown by in-gel fluorescence, and cathepsin X/L immunoblot. Actin was used as a loading control. (B) Densitometry of 35, 27, and 23 kDa bands detected by cathepsin L immunoblot, displayed as average intensity for all WT (*hBIM*) and *Ctsz*$^{-/-}$ cells relative to WT (*hBIM*) cells (fold-change). Statistics were performed using the Brown–Forsythe and Welch ANOVA tests. *n* = 3 (C–D) Mutu DCs or RAW264.7 cells were pretreated with 50 µM Biotin-Hex-Nle-SY overnight. Residual cathepsin X activity was measured with sCy5-Nle-SY. Total cathepsin X/L expression

that its intracellular accumulation is not due to impaired secretion and further confirm that total cathepsin L is increased upon loss of cathepsin X.

Collectively, these results suggest that cathepsin X regulates cathepsin L levels in an activity-dependent manner and that this effect is not likely through direct proteolysis or due to alterations in mRNA expression, glycosylation, or secretion. It is conceivable that the observed changes in oxidative stress or pH could influence cathepsin L processing or stability.

2.4 Nuclear cathepsin L is influenced by cathepsin X activity

In addition to secretion, cathepsin L is known to be trafficked to the nucleus in an importin β-dependent manner (Burton et al. 2017b). We used immunofluorescence to examine the localisation of cathepsin X and cathepsin L in Mutu DCs. Cathepsin X staining was punctate in the cytoplasm (most likely endolysosomal) but excluded from the nucleus, while cathepsin L could be observed across both compartments (Figure 4A and B). Moreover, compared to WT cells, *Ctsz*$^{-/-}$ Mutu DCs contained significantly less nuclear cathepsin L (0.93-fold, $p = 0.0002$) (Figure 4C).

Like Mutu DCs, HSC-3 human oral squamous carcinoma cells exhibit high levels of nuclear cathepsin L, but very little nuclear cathepsin X (Supplementary Figure S3A-B). Treatment with the cathepsin X inhibitor Biotin-Hex-Nle-SY resulted in significantly less nuclear cathepsin L level compared to vehicle-treated cells (0.83-fold, $p < 0.0001$) (Supplementary Figure S3C). Thus, in cell lines of completely different origins, loss of cathepsin X activity leads to less nuclear cathepsin L.

To evaluate this observation more robustly, we fractionated the nucleus and cytoplasm of Mutu DCs and examined the localisation of several lysosomal proteases. The purity of the cytoplasmic and nuclear fractions was confirmed by tubulin and lamin A, respectively. Cathepsin L was present in both the cytoplasmic and nuclear fractions (Figure 4D). Consistent with our previous data, cathepsin L was present mainly in its heavy-chain form in the cytoplasmic fraction of WT cells (Figure 4D). Cathepsin X-deficient cells exhibited an accumulation of cathepsin L single chain in the cytoplasmic fraction. In the nuclear fraction, only heavy chain cathepsin L was present regardless of the presence of cathepsin X (Figure 4D). Moreover, we observed a significant reduction in nuclear cathepsin L in cathepsin X-deficient DCs compared to WT (0.23-fold, $p = 0.0028$, Figure 4D and E). This effect was rescued by re-expression of WT and RGD mutant, but not catalytically dead cathepsin X-deficient cells. Thus, in the absence of active cathepsin X, cathepsin L single chain accumulates in the cytoplasm while nuclear levels of its heavy chain are reduced.

We also investigated the nuclear localisation of other lysosomal proteases with respect to cathepsin X. Cathepsin B and X were mainly in the cytoplasmic (lysosome-containing) fraction and absent in the nuclear fraction (Supplementary Figure S4A and B). Cathepsin H, S and legumain were observed in both cytoplasmic and nuclear fractions. Legumain was found in the nucleus in its mature form (Supplementary Figure S4B), while nuclear Cathepsin S was slightly heavier than its mature cytoplasmic form (Supplementary Figure S4C). Nuclear cathepsin H was only present in its single-chain form (Supplementary Figure S4C). Loss of cathepsin X did not affect the nuclear levels of cathepsin S/H or legumain, suggesting cathepsin X selectively regulates nuclear cathepsin L.

2.5 Processing of nuclear cathepsin L substrates is regulated by cathepsin X and legumain

As legumain also alters the processing of cathepsin L (Maehr et al. 2005), we examined cathepsin L localisation in DCs after treatment with a legumain inhibitor, SD-134. Legumain inhibition led to a pronounced accumulation of the cathepsin L single chain and loss of the heavy chain in the cytoplasmic fraction (Figure 5A). Moreover, legumain inhibition significantly reduced nuclear cathepsin L levels (0.60-fold, $p = 0.0243$), albeit to a lesser extent than cathepsin X deficiency (0.33-fold, $p = 0.0186$; Figure 5A and B). Inhibiting legumain activity in the context of cathepsin X deficiency further augmented cathepsin L single chain accumulation and reduced nuclear cathepsin L levels (0.18-fold, $p = 0.0032$, Figure 5A and B).

As nuclear cathepsin L has been shown to cleave lamin B1 (Islam et al. 2022), we subsequently examined lamin B1 processing. Cleaved lamin B1 (25 kDa) was significantly reduced in cells lacking nuclear cathepsin L due to cathepsin

was shown by immunoblot. Actin immunoblot was used as a loading control. (E–F) Densitometry of 35, 27, and 23 kDa bands detected by cathepsin L immunoblot in Mutu DCs or RAW264.7 cells, displayed as average intensity for all vehicle- and inhibitor-treated cells relative to vehicle-treated cells (fold-change). Statistics were performed using unpaired Student's *t*-tests. Three technical replicates for each condition are shown, representative of at least three independent experiments. Error bars represent SEM. ns $p > 0.05$, *$p \le 0.05$, **$p \le 0.01$, ***$p \le 0.001$, ****$p \le 0.0001$.

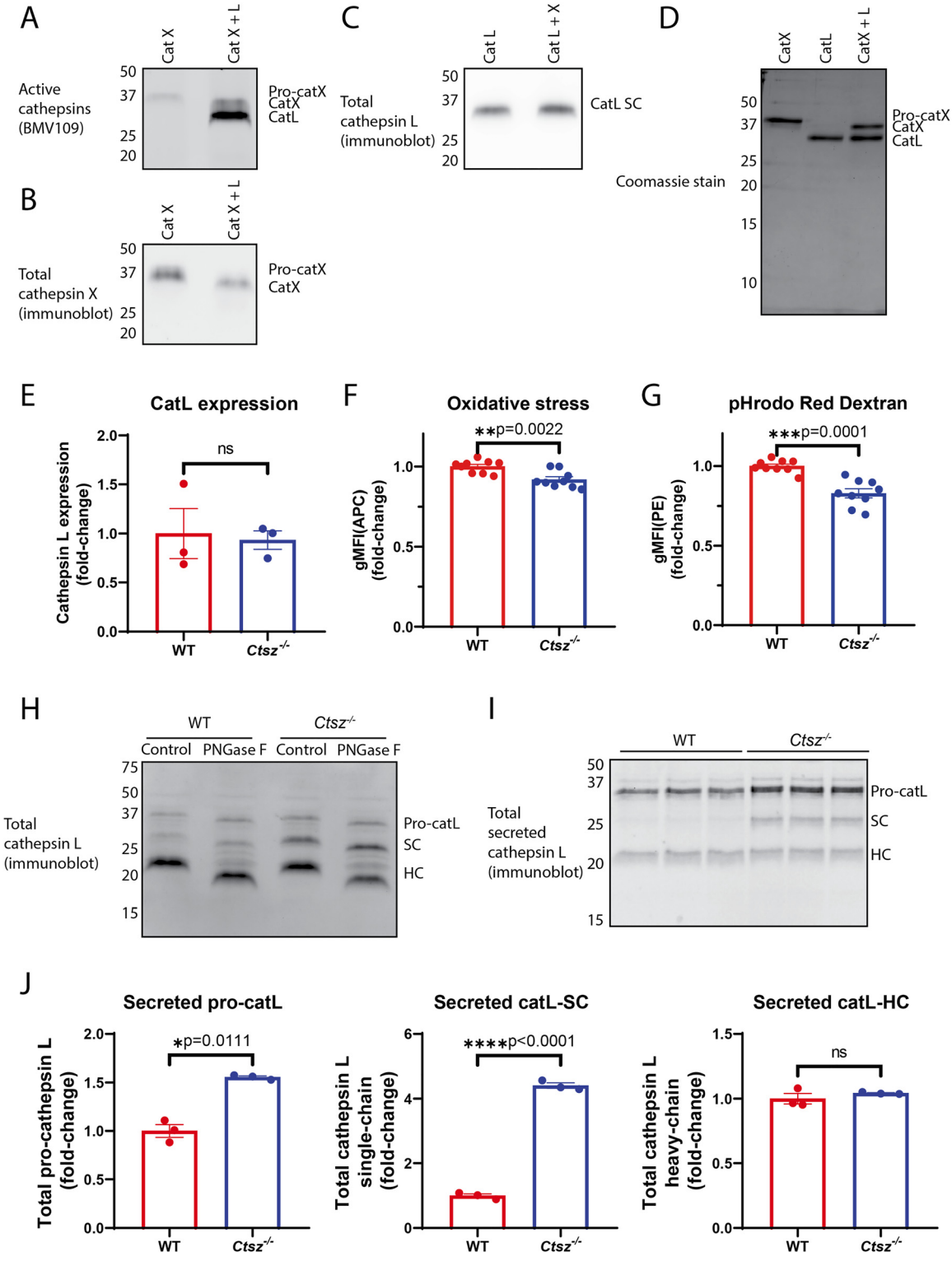

Figure 3: Accumulation of intracellular cathepsin L single chain was not due to a lack of direct cleavage by cathepsin X, lysosomal oxidative stress, glycosylation, or inhibition of cathepsin L secretion. (A) Activity of recombinant pro-cathepsin X before and after incubation with cathepsin L single chain, as shown by BMV109-labeling and in-gel fluorescence. (B) Immunoblot of cathepsin X before and after incubation with cathepsin L. Immunoblot (C) and (D) Coomassie stain of recombinant cathepsin L before and after incubation with cathepsin X. (E) Quantitative PCR analysis of cathepsin L mRNA normalised to mouse GAPDH in WT (*hBIM*) and *Ctsz*$^{-/-}$ Mutu DCs relative to WT (*hBIM*) cells (fold-change). $n = 3$. (F) Quantification of lysosomal oxidative stress using CellROX™ Deep Red Reagent in *Ctsz*$^{-/-}$ Mutu DCs relative to WT (*hBIM*; fold change). Pooled from three individual experiments with three

X deficiency (0.44-fold, p = 0.0252), legumain inhibition (0.75-fold, $p > 0.05$) or both (0.35-fold, p = 0.0285; Figure 5A and C). Overall, these results suggest that the activity of lysosomal proteases can regulate proteolysis of nuclear substrates.

3 Discussion

In this study, we assessed the impact of cathepsin X deficiency on selected lysosomal proteases and their inhibitors. Among all the proteases and endogenous inhibitors that we examined, cathepsin L was the only protease altered by cathepsin X deficiency. Specifically, we observed accumulation of the cathepsin L pro-form and single chain in the absence of cathepsin X, and this effect was dependent on the catalytic activity of cathepsin X but not its integrin-binding motif. Although previous studies have revealed context-dependent changes in cathepsin B levels in the absence of cathepsin X, with synergistic effects often observed in double knockouts (Bernhardt et al. 2010; Schwenck et al. 2019; Sevenich et al. 2010; Tamhane et al. 2014; Vasiljeva et al. 2006), we did not observe this phenomenon in Mutu DCs. As C-terminomics methods become more widely available, it will be critical to examine the overlap in physiological substrates of these two proteases in attempt to explain potential redundancies and how this differs across cell and tissue types.

Cathepsin L processing from the single chain into its two-chain form is known to be legumain dependent, as both legumain inhibition and genetic deletion results in the accumulation of cathepsin L single chain and concomitant loss of its heavy chain (Anderson et al. 2020; Edgington-Mitchell et al. 2015, 2016; Maehr et al. 2005; Shirahama-Noda et al. 2003). Indeed, treatment of Mutu DCs with a legumain inhibitor resulted in single chain accumulation and loss of heavy chain (Figure 5C). In the context of cathepsin X deficiency, however, legumain expression and activity were not altered, suggesting that cathepsin X does not regulate cathepsin L processing through effects on legumain activity. Moreover, cathepsin X deficiency led to increased cathepsin L single chain without affecting its heavy chain. These results suggest that legumain and cathepsin X may regulate cathepsin L through distinct mechanisms.

Cathepsin X is an exopeptidase that cleaves one amino acid at a time from the carboxy terminus of its substrates. Cathepsin B, the cathepsin most similar to cathepsin X, is primarily a dipeptidyl carboxypeptidase (DPCP) but also exhibits endopeptidase activity (Yoon et al. 2022). Using a recombinant protein cleavage assay, we queried whether cathepsin X may have potential endopeptidase activity to process the cathepsin L. Cathepsin X did not directly cleave cathepsin L single chain to its two-chain form. Thus, while cathepsin X activity may promote the conversion, it is not likely driven by direct cleavage.

We next sought alternative explanations for the increased total level of cathepsin L in cathepsin X-deficient cells. We first hypothesised that the expression of cathepsin L was increased due to lysosomal oxidative stress, as has been shown previously to drive STAT3-dependent transcription of lysosomal enzymes (Martínez-Fábregas et al. 2018). However, loss of cathepsin X did not provoke oxidative stress or increase cathepsin L mRNA. In fact, oxidative stress was slightly decreased in *Ctsz*$^{-/-}$ cells, and the endolysosomal pH was increased. We also questioned whether cathepsin X deficiency altered cathepsin L secretion and resulted in accumulation of single chain in the cytoplasm. On the contrary, cathepsin X-deficient cells secreted more cathepsin L pro-form and single chain, affirming that total cathepsin L is increased in the absence of cathepsin X. It is possible that the observed changes in oxidative environment and pH would lead to stabilisation of cathepsin L single chain, but further studies will be required in future to investigate this in more detail.

While the mechanisms by which cathepsin X regulates cathepsin L remain poorly understood, we instead turned our attention to identifying possible consequences of this interaction. Ultimately, we demonstrated that nuclear cathepsin L was reduced upon loss of cathepsin X, and this resulted in less processing of lamin B1, a known cathepsin L substrate. This effect was mirrored in wild-type cells treated with a legumain inhibitor, and legumain inhibition further augmented the effect in cathepsin X-deficient cells. In wild-type Mutu DCs, nuclear cathepsin L is predominantly found in the heavy chain form; this was observed previously in ARCaP-M and HCT116 cells (Burton et al. 2017a; Tamhane et al. 2016). Surprisingly, loss of cathepsin X led to reduced nuclear heavy chain, despite similar levels of cytoplasmic

replicates each. (G) pHrodo red fluorescence in *Ctsz*$^{-/-}$ Mutu DCs relative to WT (*hBIM*; fold change). Pooled from three individual experiments with three replicates each. (H) Lysates from WT (hBIM) or *Ctsz*$^{-/-}$ Mutu DCs were pretreated with PNGase F and immunoblotted for cathepsin L. (I) Cathepsin L secretion in WT (*hBIM*) and *Ctsz*$^{-/-}$ Mutu DCs, as shown by cathepsin L immunoblot. Three technical replicates of bulk-sorted clones for each condition are shown, representative of at least three independent experiments. (J) Densitometry of secreted 35, 27, and 23 kDa species detected by cathepsin L immunoblot, displayed as average intensity for all WT (*hBIM*) and *Ctsz*$^{-/-}$ cells relative to WT (fold-change). Statistics were performed using unpaired Student's *t*-tests. n = 3. Error bars represent SEM. ns $p > 0.05$, *$p \leq 0.05$, **$p \leq 0.01$, ***$p \leq 0.001$, ****$p \leq 0.0001$.

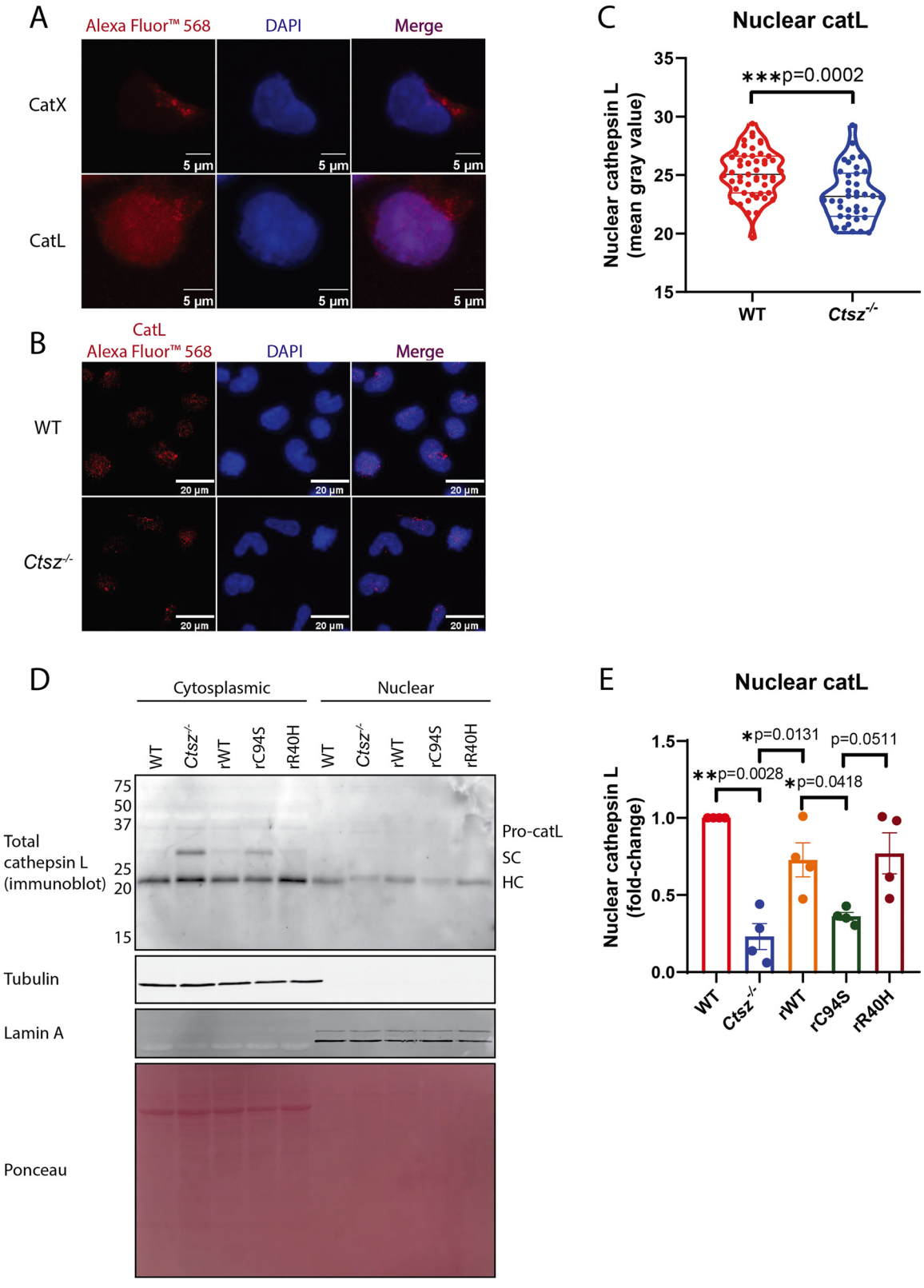

Figure 4: Nuclear cathepsin L is regulated by cathepsin X activity. (A) Intracellular cathepsin X/L in Mutu DCs as shown by immunofluorescence. Scale bar = 5 µm. (B) Intracellular cathepsin L in Mutu DCs as shown by immunofluorescence. Scale bar = 20 µm. (C) Quantification of nuclear cathepsin L in Mutu DCs (n = 51 WT cells vs. n = 38 *Ctsz*$^{-/-}$ cells). Statistics were performed using unpaired Student's t-tests. (D) Cathepsin L immunoblot in the cytoplasmic and nuclear fractions of WT (*hBIM*) and *Ctsz*$^{-/-}$ Mutu DCs and *Ctsz*$^{-/-}$ cells re-expressing WT, rC94S, or rR40H cathepsin X. Tubulin expression was used as a cytoplasmic marker and loading control. Lamin A expression was used as a nuclear marker and loading control. (E) Densitometry analysis of nuclear 23 kDa bands detected by cathepsin L immunoblot, displayed as average intensity normalised to WT (*hBIM*) (fold change). Statistics were performed using unpaired Student's t-tests. n = 3.

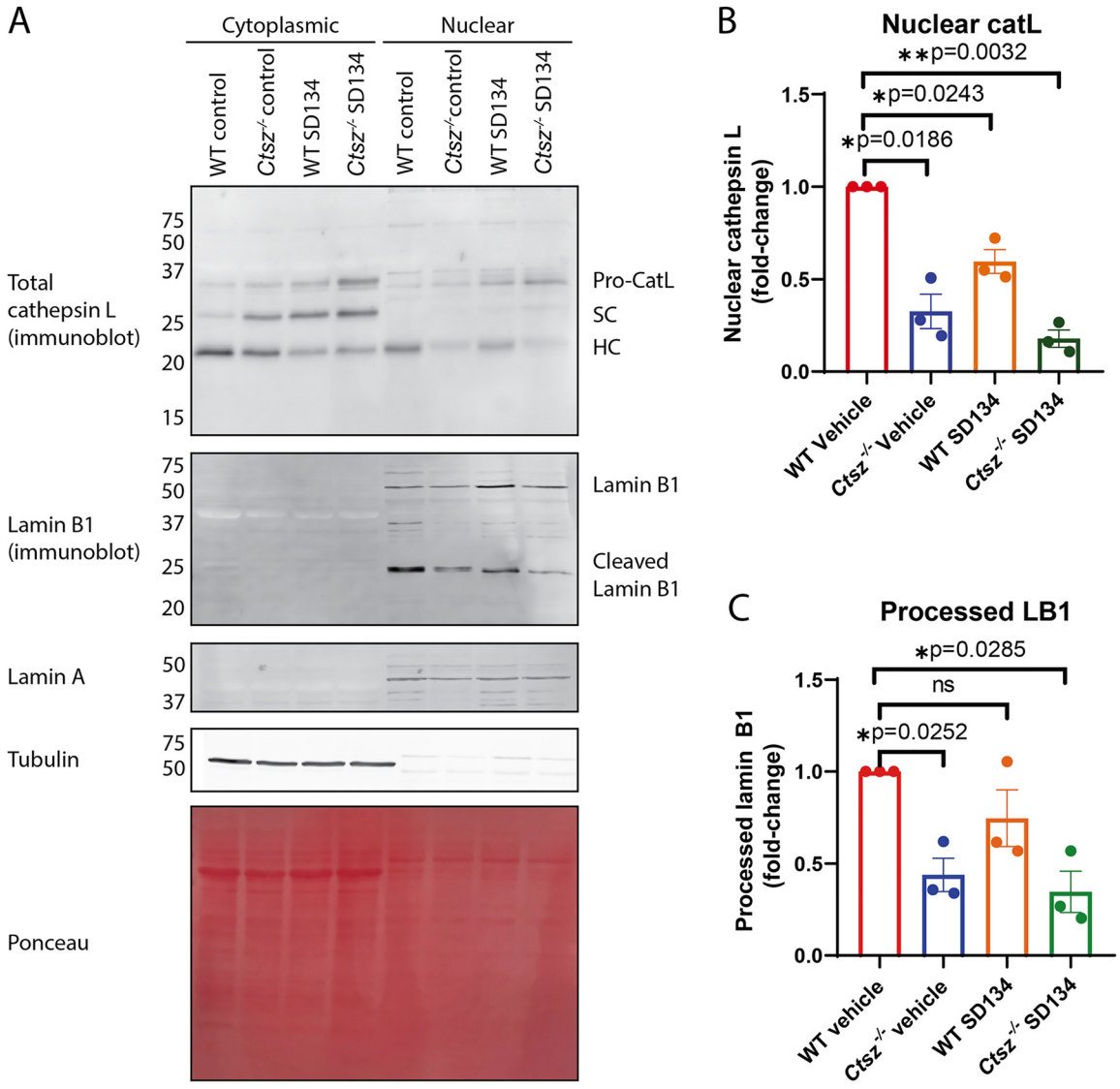

Figure 5: Cathepsin X deficiency impaired cathepsin L nuclear localisation and nuclear proteolysis. (A) Cathepsin L and lamin B1 immunoblot in the cytoplasmic fraction and nuclear fraction in WT (*hBIM*) or *Ctsz*$^{-/-}$ cells treated with or without legumain inhibitor SD-134 (100 µM). Tubulin expression was used as a cytoplasmic marker and loading control. Lamin A expression was used as a nuclear marker and loading control. Ponceau stain was used as a second measure of protein loading. (B) Densitometry analysis of nuclear 23 kDa bands detected by cathepsin L immunoblot, displayed as average intensity normalised to WT (*hBIM*) control (fold change). Statistics were performed using unpaired Student's *t*-tests. $n = 3$. Error bars represent SEM. (C) Densitometry analysis of processed lamin B1 (25 kDa) detected by lamin B1 immunoblot, displayed as average intensity normalised to WT (*hBIM*) control (fold change). Statistics were performed using unpaired Student's *t*-tests. $n = 3$. Error bars represent SEM. ns $p > 0.05$, *$p \leq 0.05$, **$p \leq 0.01$, ***$p \leq 0.001$, ****$p \leq 0.0001$.

heavy chain. This suggests that cathepsin X may function to promote translocation of cathepsin L to the nucleus. One possible explanation is that cathepsin X promotes lysosomal membrane permeabilisation (LMP). As recently hypothesised by Reinheckel (Reinheckel and Tholen 2022), LMP could permit release of cathepsin L into the cytosol and its transport to the nucleus. The observed increase in oxidative stress and lowered pH when cathepsin X is present may function to promote LMP, although whether/how this occurs will require further investigation.

Burton et al. demonstrated that cathepsin L is transported to the nucleus in an importin β1-dependent manner (Burton et al. 2017b). This translocation depends on binding of cathepsin L to snail, which contains a nuclear localisation sequence. It is also conceivable that cathepsin X somehow regulates the interaction between snail and cathepsin L.

Alternatively, lysosomal and nuclear cathepsin L levels have been shown to vary with cell cycle stages in HCT116 cells, with the highest levels observed during S phase (Tamhane et al. 2016). It may be possible that cathepsin X influences cell cycle progression through an unknown mechanism, leading to changes in cathepsin L abundance and distribution.

In addition to lamin B1, other nuclear substrates of cathepsin L have been reported, including CCAAT-displacement protein/cut homeobox (CDP/Cux) transcription factor (Goulet et al. 2007). Nuclear cathepsins, including L, have also been reported to cleave and stabilise histones to regulate processes such as cellular differentiation and cell cycle progression (Adams-Cioaba et al. 2011; Daura et al. 2021; Duncan et al. 2008; Sereesongsaeng et al. 2023). In the future, it will be important to more systematically investigate nuclear substrates of cathepsin L in diverse cell types, to examine whether the presence of active cathepsin X broadly influences nuclear proteolysis, and to dissect the consequential effects.

Finally, little information is known about the function of the single- and two-chain forms of cathepsins. Both forms are known to be catalytically active and can bind to the activity-based probe DCG04 (Maehr et al. 2005). It is possible that the different forms exhibit divergent substrate profiles. In support of this, the two-chain form exhibits gelatinase activity, while the single-chain form does not (Mattock et al. 2010). This suggests that shifting the balance of the two forms in response to cathepsin X inhibition or deletion may have significant effects on not only the degree and location of cathepsin L proteolysis, but also on its repertoire of substrates. This shift may also occur in the setting of disease; indeed, accumulation of single-chain cathepsin L has been observed in the hippocampus of patients with Alzheimer's disease compared to healthy controls (Islam et al. 2022).

In summary, we have evaluated the relationship between cathepsin X and other lysosomal cysteine cathepsins, legumain, and cystatins in murine dendritic cells, observing a selective influence on cathepsin L. These findings will inform future studies on the downstream impacts of both cathepsin X and L proteolysis in the context of health and disease.

4 Materials and methods

4.1 Cell culture

Mutu DCs (Fuertes Marraco et al. 2012) and Mutu Cas9 DCs (Wilson et al. 2018) were cultured in Iscove's Modified Dulbecco's Medium (IMDM; Gibco; Scoresby, Australia) supplemented with 10 % (v/v) fetal bovine serum (FBS), 60 µg/mL penicillin, 100 µg/mL streptomycin and 100 µM β-mercaptoethanol (Fuertes Marraco et al. 2012; Wilson et al. 2018). To passage, Mutu DCs were lifted from the flask using ethylenediaminetetraacetic acid-balanced salt solution (EDTA-BSS; 150 mM sodium chloride, 4 mM potassium chloride, 24 µM disodium hydrogen orthophosphate, 12 µM sodium dihydrogen orthophosphate, 15 mM HEPES, and 5 mM EDTA (The Peter Doherty Institute for Infection and Immunity media preparation unit [MPU]; Melbourne, Australia) supplemented with 2 % (v/v) FBS). RAW264.7 cells were cultured in Dulbecco's Modified Eagle Medium (DMEM; Gibco) supplied with 10 % (v/v) FBS and 1 % (v/v) antibiotic-antimycotic. RAW264.7 cells were lifted from the flasks using a rubber policeman. HSC-3 cells were cultured in Dulbecco's Modified Eagle Medium (DMEM; Gibco) supplied with 10 % (v/v) FBS and 1 % (v/v) antibiotic-antimycotic (Momose et al. 1989). HSC-3 cells were lifted using trypsin (1.25 %). All cells were maintained in humidified incubators at 37 °C and 5 % CO_2.

4.2 Detection of protease activity using activity-based probes and in-gel fluorescence

The following activity-based probes were dissolved in DMSO and added to the cell media 4 h before harvesting (final concentration 1 µM, 0.1 % DMSO): sCy5-Nle-SY (cathepsin X and S selective) (Mountford et al. 2020), BMV109 (cathepsin X, B, S, L) (Edgington-Mitchell et al. 2017; Verdoes et al. 2013), FY01 (cathepsin C) (Yuan et al. 2006), or LE28 (legumain) (Edgington et al. 2013). Cells were collected, washed with PBS to remove excess probe and serum, and lysed with PBS containing 0.1 % Triton X-100. Cell lysates were cleared of debris by centrifugation at max speed for 7 min, and supernatants were transferred to a new tube. A BCA assay (Thermo Fisher; Scoresby, Australia) was used to determine the total protein concentration using FLUOstar® (BMG LABTECH; Mornington, Australia). Sample buffer (1X: 10 % glycerol, 50 mM Tris-Cl, pH 6.8, 2 % SDS, 0.01 % bromophenol blue, 1.25 % beta-mercaptoethanol) was added to each sample from a 5X stock, followed by a 5 min boiling at 95 °C. Equal protein amounts (in general 80 µg) were resolved on 15 % SDS-PAGE gels poured in-house. The gels were scanned for Cy5 fluorescence using a Typhoon 5 (GE Healthcare; Parramatta, Australia).

4.3 Small molecule protease inhibitors

Small molecule protease inhibitors, including Biotin-Hex-Nle-SY (50 µM; see supplementary methods for synthetic details) and SD-134 (100 µM) (Lee and Bogyo 2012), were administered directly into cell media (0.1 % final DMSO) and incubated for 24 h prior to assessment of residual protease activity as above.

4.4 Analysis of conditioned media

Cells were washed with and plated in serum-free media (1×10^6 cells/well in 6-well plates) and media was conditioned for 24 h. Conditioned media (CM) was collected, centrifuged at 300 g for 5 min to remove cell debris, and concentrated using Amicon® Ultra 0.5 mL 3 kDa (Millipore; Bayswater, Australia) centrifugal filters according to the manufacturer's instructions. A BCA assay was used to determine the total protein concentration using FLUOstar® (BMG LABTECH). A total of ~80 µg protein was resolved on 15 % SDS-PAGE.

4.5 Immunoblotting

Proteins were transferred from gels to nitrocellulose membranes using a Trans-Blot Turbo Transfer System (BioRad; South Granville, Australia) in transfer buffer (1× Trans-Blot® Turbo™ Transfer Buffer [BioRad] containing 20 % ethanol). Membranes were incubated in primary antibodies overnight at 4 °C: cathepsin X (AF1033, R&D Systems; Minneapolis, United States), cathepsin S (AF1183, R&D Systems), cathepsin B (AF965, R&D Systems;), cathepsin L (AF1515, R&D Systems), cathepsin H (AF1013, R&D Systems), cystatin C (AF1238, R&D Systems), stefin A (ab61223, Abcam; Melbourne, Australia) and stefin B (ab92449, Abcam), all diluted at 1:1000. β-Actin (MA5-15739, Life Technologies; Mulgrave, Australia), tubulin (A5060, Sigma Aldrich; Bayswater, Australia), lamin B1 (33–2000, Invitrogen; Mt Waverley, Australia) or lamin A (L1293, Sigma Aldrich), all diluted at 1:10 000. Membranes were washed with PBS containing 0.05 % Tween-20 (PBST) three times followed by incubation with secondary antibody on an orbital shaker for 1 h at room temperature: donkey anti-goat HRP (A15999, Invitrogen), and donkey anti-rabbit IRDye 800CW (92632213, Licor; Lincoln, United States), all diluted at 1:10 000. The membrane was then washed three times using PBST and once with PBS. IR800 immunoblots were scanned using Typhoon 5 (GE Healthcare). HRP labelling was visualised on a ChemiDoc® MP imager (BioRad; South Granville, Australia) using Pierce ECL Western blotting reagents (Thermo Fisher).

4.6 Immunofluorescence

Chamber slides (Ibidi, 80826; Gräfelfing, Germany) were washed twice with 250 µL PBS and once with 250 µL IMDM. Cells (25 000) were added to each chamber in 250 µL media and incubated overnight. The attached cells were washed with 150 µL PBS twice and fixed with 150 µL 4 % paraformaldehyde in PBS at room temperature for 10 min. Cells were then permeabilised with 150 µL 0.1 % Triton X-100 at room temperature for 3 min, washed with PBS, and blocked with 10 % normal horse serum (NHS) in PBS at room temperature for 30 min. Primary antibody diluted in 150 µL blocking buffer (1:200) was added to each chamber and incubated at 4 °C overnight. Cells were washed twice with 150 µL 0.1 % Triton X-100 in PBS followed by addition of secondary antibody (donkey anti-goat 568, A-11057, Thermo Fisher; diluted 1:1000 in blocking buffer) at room temperature for 1 h. Cells were washed twice with 150 µL 0.1 Triton X-100 in PBS and nuclei were stained with DAPI in PBS (1 µg/mL) at room temperature for 5 min. After washing with PBS 3 times, cells were stored in mounting buffer (90 % Glycerol in PBS) and imaged using the Leica SP8 Confocal Microscope (Leica; Macquarie Park, Australia) with a 63×/1.40 oil objective.

Nuclear cathepsin L was quantified using ImageJ. Briefly, the nucleus (region of interest) was selected using the "Analyse Particles" function. The intensity of nuclear cathepsin L staining was subsequently measured within the region of interest.

4.7 Oxidative stress and pH

Cells (100,000) were seeded in 96-well plates and treated with pHrodo Red Dextran (20 µg/mL, Invitrogen P35368, Scoresby, Australia) or CellRox (5 µM, Invitrogen C10422, Carlsbad, United States) at 37 °C for 30 min. Cells were washed with BSS-EDTA 2 % FBS followed by centrifugation at 1700 rpm for 2 min twice. Propidium iodide (PI) (0.5 µg/mL, Calbiochem® 537059, Bayswater, Australia) was diluted in BSS-EDTA 2 % FBS and added to differentiate live/dead cells. Sample acquisition was conducted on L.S.R. Fortessa (BD Bioscience). Data analysis was performed using FlowJo V10.0.7 (TreeStar, Inc.). Mean fluorescence intensity (MFI) is reported relative to WT cells (fold-change), and data were pooled from three independent experiments, each with three technical replicates.

4.8 CRISPR-Cas9

Cathepsin X (guide RNA TTGCTACCATCCCATTCGCG) knockout/knockdown cell lines were generated using the CRISPR/Cas9 system. Cells transduced with guide RNA targeting the human BCL2-like gene (*hBIM*; guide RNA GCCCAAGAGTTGCGGCGTAT), which is not found in the mouse genome, were generated as a negative control. *hBIM* cells should not have undergone genome editing but were exposed to the same conditions as the cathepsin X knockout cells. Details of the method are reported in the supplementary material.

4.9 Cathepsin X re-expression

Three constructs of murine cathepsin X cDNA cloned into the puc57 vector were purchased from Biomatik (Wilmington, United States): WT cathepsin X, catalytically dead cathepsin X (C94S), and integrin-binding mutant cathepsin X (R40H). Without changing the amino acid sequence, the EcoRI restriction site was mutated within all three constructs from GAATTC to GAGTTC. The PAM sequence following the guide RNA target site was mutated from GGG to GTG. Subsequently, the three cathepsin X variants were amplified by PCR with primers generating Gibson Assembly overhangs (5′ overhang: 5′-CCTTCTCTAGGCGCCGGCCGGATCC-3′; 3′ overhang: 5′ GTCGACCCTGTGGAATGTGTGTCAG-3′).

According to the manufacturer's protocol, the purified PCR products were cloned into the retroviral pBABE-puro vector with the Gibson Assembly kit (NEB; Notting Hill, Australia). According to the manufacturer's protocol, pBABE vectors were transfected into HEK293T cells along with pGag-pol and pVSV-G vectors with Lipofectamine 3000 (Thermo Fisher). The resulting viral supernatant was then used to infect Mutu DCs by adding 8 µg/mL polybrene for 24 h. The transduced cells were then selected with 1 µg/mL puromycin.

4.10 RNA isolation, cDNA synthesis and quantitative real-time PCR

Total RNA was extracted using Trizol, and genomic DNA was removed using DNase (Thermno Scientific, EN0521). cDNA was synthesized using a kit (Promega, A5001; Alexandria, Australia). All primers were designed using Primer 3 (National Center for Biotechnology Information) and verified by Primer Blast (NIH). GAPDH (F, 5′-GGTGCTGAGTATGTCGTGGA-3′; R, 5′-CGGAGATGATGACCCTTTTG-3′) was used as a house keeping gene control; cathepsin X (F, 5′-GGATTGTCCGAAATTCATGG-3′; R, 5′-ACTCTCGATGGCAAGGTTGT-3′) and cathepsin L (F, 5′-AGAGTAGCACCAGTGGAAGT-3′; R, 5′-CCGTTGTGTAGCTGGATCATT-3′) were amplified with the QuantStudio™ 6 system (Thermo Fisher) using the following PCR conditions: 95 °C for 3 min; 45 cycles of 95 °C for 15 s and 60 °C for 20 s. All mRNA levels were presented relative to GAPDH. Further details are reported in the supplementary materials.

4.11 Nuclear fractionation

Cells were seeded in 10 cm dishes. When confluent, cells were collected and lysed with 200 µL cytoplasmic buffer (10 mM HEPES, 1.5 mM MgCl2, 10 mM KCl, 0.5 mM DTT, and 0.05 % NP40) followed by centrifugation at 4 °C, 3000 rpm for 10 min. The supernatant containing the cytoplasmic fraction was collected. The remaining pellets containing nuclear fractions were dissolved with 50 µL nuclear buffer (5 mM HEPES, 1.5 mM $MgCl_2$, 0.2 mM EDTA, 0.5 mM DTT, 26 % glycerol (v/v), and 300 mM NaCl), followed by sonicating twice at 40 % amp (QSONICA Q500; Newtown, United States) for 10 s. The homogenate was left on ice for 30 min, followed by centrifugation at max speed for 20 min at 4 °C. Supernatants containing the nuclear fraction were collected. For cytoplasmic proteins, an equal protein amount (in general 80 µg) was resolved on 15 % SDS-PAGE gels poured in-house. The nuclear protein samples were loaded at the same volume as their corresponding cytoplasmic samples and were 4 times more concentrated. The purity of the cytoplasmic and nuclear fractions was assessed by blotting for tubulin and lamin A, respectively, as above.

4.12 Recombinant protease cleavage assay

Recombinant proteases (cathepsin X, 934-CY, R&D Systems; cathepsin L 952-CY, R&D Systems; 500 ng each) were dissolved in 50 mM sodium acetate and 500 mM sodium chloride [pH 5.5] and incubated at 37 °C for 1 h. Where indicated, 1 µM BMV109 was added and incubated for 20 min. Sample buffer (5X) was added to each sample, followed by boiling at 95 °C for 5 min. Samples were resolved on 15 % SDS-PAGE gels poured in-house. The gels were scanned on a Typhoon 5 (if required), transferred, and immunoblotted as above. Alternatively, they were stained with 0.5 % Brilliant Blue (Sigma), 50 % methanol, and 10 % acetic acid for 30 min, followed by washing three times with destain buffer (30 % ethanol, 10 % acetic acid) on an orbital shaker for 10 min. Gels were further washed in water on an orbital shaker overnight. Coomassie-stained proteins were imaged with an IRLong filter on a Typhoon 5 (GE Healthcare).

4.13 Statistical analysis

Statistical analyses were performed using GraphPad Prism 8. Unpaired *t*-tests were performed to analyse differences between two groups. Ordinary one-way ANOVA followed by Dunnett's multiple comparisons test was used to compare more than two groups where indicated. Mean data points were expressed as mean ± SEM. $p < 0.05$ was considered significant.

Acknowledgments: We thank Gerry Healey from the Mintern Lab for helping with the CRISPR-Cas9 process, the D. Stroud Lab for providing vectors and materials for protein re-expression, M. Harold for providing vectors, the Biological Optical Microscopy Platform at the Bio21 Institute, the Australian Genome Research Facility at the Peter MacCallum Cancer Centre, and the flow cytometry platform at the Murdoch Children's Research Institute.

Research ethics: No animal or human ethics approval was required to complete this work.

Author contributions: B.X. Conceptualization; Data curation; Formal analysis; Investigation; Methodology; Validation; Writing – original draft. B.M.A. Investigation; Methodology; Project administration; Writing – review & editing. S.J.M. Data curation; Methodology; Writing – review & editing. P.E.T. Resources; Supervision. J.D.M. Conceptualization; Resources; Supervision; Writing – review & editing. L.E.E.-M. Conceptualization; Funding acquisition; Investigation; Methodology; Project administration; Resources; Supervision; Writing – review & editing.

Competing interests: The authors declare no competing interests.

Research funding: This work was supported by a Grimwade Research Fellowship funded by the Russell and Mab Grimwade Miegunyah Fund, an Australian Research Council DECRA fellowship (DE180100418), and a National Health and Medical Research Council Ideas Grant (GNT2011119) awarded to L.E.E.-M.

Data availability: All data are available upon request.

References

Adams-Cioaba, M.A., Krupa, J.C., Xu, C., Mort, J.S., and Min, J. (2011). Structural basis for the recognition and cleavage of histone H3 by cathepsin L. *Nat. Commun.* 2: 197.

Akkari, L., Gocheva, V., Kester, J.C., Hunter, K.E., Quick, M.L., Sevenich, L., Wang, H.W., Peters, C., Tang, L.H., Klimstra, D.S., et al. (2014). Distinct functions of macrophage-derived and cancer cell-derived cathepsin Z combine to promote tumor malignancy via interactions with the extracellular matrix. *Genes Dev*. 28: 2134–2150.

Allan, E.R.O., Campden, R.I., Ewanchuk, B.W., Tailor, P., Balce, D.R., McKenna, N.T., Greene, C.J., Warren, A.L., Reinheckel, T., and Yates, R.M. (2017). A role for cathepsin Z in neuroinflammation provides mechanistic support for an epigenetic risk factor in multiple sclerosis. *J. Neuroinflammation*. 14: 1–11.

Anderson, B.M., de Almeida, L.G.N., Sekhon, H., Young, D., Dufour, A., and Edgington-Mitchell, L.E. (2020). N-Terminomics/TAILS of after after chemical inhibition of legumain. *Biochem*. 59: 329–340.

Bernhardt, A., Kuester, D., Roessner, A., Reinheckel, T., and Krueger, S. (2010). Cathepsin X deficient gastric epithelial cells in co-culture with macrophages: characterization of cytokine response and migration capability after Helicobacter pylori infection. *J. Biol. Chem.* 285: 33691–33700.

Burton, L.J., Dougan, J., Jones, J., Smith, B.N., Randle, D., Henderson, V., and Odero-Marah, V.A. (2017a). Targeting the L CCAAT displacement protein/cut homeobox transcription factor-epithelial mesenchymal transition pathway in prostate and breast cancer cells with the Z-FY-CHO inhibitor. *Mol. Cell. Biol.* 37: 002977–16.

Burton, L.J., Henderson, V., Liburd, L., and Odero-Marah, V.A. (2017b). Snail transcription factor NLS and importin β1 regulate the subcellular localization of cathepsin L and Cux1. *Biochem. Biophys. Res. Commun.* 491: 59–64.

Campden, R.I., Warren, A.L., Greene, C.J., Chiriboga, J.A., Arnold, C.R., Aggarwal, D., McKenna, N., Sandall, C.F., MacDonald, J.A., and Yates, R.M. (2022). Extracellular cathepsin Z signals through the α(5) integrin and augments NLRP3 inflammasome activation. *J. Biol. Chem.* 298: 101459.

Chapman, H.A., Riese, R.J., and Shi, G.P. (1997). Emerging roles for cysteine proteases in human biology. *Annu. Rev. Physiol.* 59: 63–88.

Dahl, S.W., Halkier, T., Lauritzen, C., Dolenc, I., Pedersen, J., Turk, V., and Turk, B. (2001). Human recombinant pro-dipeptidyl peptidase I (cathepsin C) can be activated by cathepsins L and S but not by autocatalytic processing. *Biochem*. 40: 1671–1678.

Daura, E., Tegelberg, S., Yoshihara, M., Jackson, C., Simonetti, F., Aksentjeff, K., Ezer, S., Hakala, P., Katayama, S., Kere, J., et al. (2021). Cystatin B-deficiency triggers ectopic histone H3 tail cleavage during neurogenesis. *Neurobiol. Dis.* 156: 105418.

Deussing, J., von Olshausen, I., and Peters, C. (2000). Murine and human cathepsin Z: cDNA-cloning, characterization of the genes and chromosomal localization. *Biochim. Biophys. Acta - Gene Structure and Expression* 1491: 93–106.

Duncan, E.M., Muratore-Schroeder, T.L., Cook, R.G., Garcia, B.A., Shabanowitz, J., Hunt, D.F., and Allis, C.D. (2008). Cathepsin L proteolytically processes histone H3 during mouse embryonic stem cell differentiation. *Cell* 135: 284–294.

Edgington, L.E., Verdoes, M., Ortega, A., Withana, N.P., Lee, J., Syed, S., Bachmann, M.H., Blum, G., and Bogyo, M. (2013). Functional imaging of legumain in cancer a quenched activity-based probe. *J. Am. Chem. Soc.* 135: 174–182.

Edgington-Mitchell, L.E., Rautela, J., Duivenvoorden, H.M., Jayatilleke, K.M., van der Linden, W.A., Verdoes, M., Bogyo, M., and Parker, B.S. (2015). Cysteine cathepsin activity suppresses osteoclastogenesis of myeloid-derived suppressor cells in breast cancer. *Oncotarget*. 6: 27008–27022.

Edgington-Mitchell, L.E., Wartmann, T., Fleming, A.K., Gocheva, V., van der Linden, W.A., Withana, N.P., Verdoes, M., Aurelio, L., Edgington-Mitchell, D., Lieu, T., et al. (2016). Legumain is activated in macrophages during pancreatitis. *Am. J. Physiol.: Gastrointest. Liver Physiol.* 311: G548–G560.

Edgington-Mitchell, L.E., Bogyo, M., and Verdoes, M. (2017). Live cell imaging and profiling of cysteine cathepsin activity using a quenched activity-based probe. *Methods Mol. Biol.* 1491: 145–159.

Fuertes Marraco, S., Grosjean, F., Duval, A., Rosa, M., Lavanchy, C., Ashok, D., Haller, S., Otten, L., Steiner, Q.-G., Descombes, P., et al. (2012). Novel murine dendritic cell lines: a powerful auxiliary tool for dendritic cell research. *Front. Immunol.* 3: 331.

Goulet, B., Sansregret, L., Leduy, L., Bogyo, M., Weber, E., Chauhan, S.S., and Nepveu, A. (2007). Increased expression and activity of nuclear cathepsin L in cancer cells suggests a novel mechanism of cell transformation. *Mol. Cancer Res.* 5: 899–907.

Hamon, Y., Legowska, M., Hervé, V., Dallet-Choisy, S., Marchand-Adam, S., Vanderlynden, L., Demonte, M., Williams, R., Scott, C.J., Si-Tahar, M., et al. (2016). Neutrophilic cathepsin C is maturated by a multistep proteolytic process and secreted by activated cells during Inflammatory lung diseases. *J. Biol. Chem.* 291: 8486–8499.

Hsing, L.C. and Rudensky, A.Y. (2005). The lysosomal cysteine proteases in MHC class II antigen presentation. *Immunol. Rev.* 207: 229–241.

Hua, Y. and Nair, S. (2015). Proteases in cardiometabolic diseases: Pathophysiology, molecular mechanisms and clinical applications. *Biochim. Biophys. Acta* 1852: 195–208.

Islam, M.I., Nagakannan, P., Shcholok, T., Contu, F., Mai, S., Albensi, B.C., Del Bigio, M.R., Wang, J.F., Sharoar, M.G., Yan, R., et al. (2022). Regulatory role of cathepsin L in induction of nuclear laminopathy in Alzheimer's disease. *Aging Cell* 21: e13531.

Jevnikar, Z., Obermajer, N., and BogyoMKos, J. (2008). The role of cathepsin X in the migration and invasiveness of T lymphocytes. *J. Cell Sci.* 121: 2652–2661.

Kos, J., Sekirnik, A., Premzl, A., Zavašnik Bergant, V., Langerholc, T., Repnik, U.k., Turk, B., Werle, B., Golouh, R., Jeras, M., et al. (2005). Carboxypeptidases cathepsins X and B display distinct protein profile in human cells and tissues. *Exp. Cell Res.* 306: 103–113.

Lee, J. and Bogyo, M. (2012). Synthesis and evaluation of aza-peptidyl inhibitors of the lysosomal asparaginyl endopeptidase, legumain. *Bioorg. Med. Chem. Lett.* 22: 1340–1343.

López-Otín, C. and Bond, J.S. (2008). Proteases: multifunctional enzymes in life and disease. *J. Biol. Chem.* 283: 30433–30437.

Mach, L., Mort, J.S., and Glössl, J. (1994). Maturation of human procathepsin B. Proenzyme activation and proteolytic processing of the precursor to the mature proteinase, in vitro, are primarily unimolecular processes. *J. Biol. Chem.* 269: 13030–13035.

Maehr, R., Hang, H.C., Mintern, J.D., Kim, Y.-M., Cuvillier, A., Nishimura, M., Yamada, K., Shirahama-Noda, K., Hara-Nishimura, I., and Ploegh, H.L. (2005). Asparagine endopeptidase is not essential for class II MHC antigen presentation but is required for processing of cathepsin L in mice. *J. Immunol.* 174: 7066–7074.

Martínez-Fábregas, J., Prescott, A., van Kasteren, S., Pedrioli, D.L., McLean, I., Moles, A., Reinheckel, T., Poli, V., and Watts, C. (2018). Lysosomal protease deficiency or substrate overload induces an oxidative-stress mediated STAT3-dependent pathway of lysosomal homeostasis. *Nat. Commun.* 9: 5343.

Mattock, K.L., Gough, P.J., Humphries, J., Burnand, K., Patel, L., Suckling, K.E., Cuello, F., Watts, C., Gautel, M., Avkiran, M., et al. (2010). Legumain and cathepsin-L expression in human unstable carotid plaque. *Atherosclerosis* 208: 83–89.

McQueney, M.S., Amegadzie, B.Y., D'Alessio, K., Hanning, C.R., McLaughlin, M.M., McNulty, D., Carr, S.A., Ijames, C., Kurdyla, J., and Jones, C.S. (1997). Autocatalytic activation of human cathepsin K. *J. Biol. Chem.* 272: 13955–13960.

Ménard, R., Carmona, E., Takebe, S., Dufour, É., Plouffe, C., Mason, P., and Mort, J.S. (1998). Autocatalytic processing of recombinant human procathepsin L. Contribution of both intermolecular and unimolecular events in the processing of procathepsin L in in vitro. *J. Biol. Chem.* 273: 4478–4484.

Mitrovic, A., Fonovic, U.P., and Kos, J. (2017). Cysteine cathepsins B and X promote epithelial-mesenchymal transition of tumor cells. *Eur. J. Cell Biol.* 96: 622–631.

Momose, F., Araida, T., Negishi, A., Ichijo, H., Shioda, S., and Sasaki, S. (1989). Variant sublines with different metastatic potentials selected in nude mice from human oral squamous cell carcinomas. *J. Oral Pathol. Med.* 18: 391–395.

Mountford, S.J., Anderson, B.M., Xu, B., Tay, E.S.V., Szabo, M., Hoang, M.-L., Diao, J., Aurelio, L., Campden, R.I., Lindström, E., et al. (2020). Application of a sulfoxonium ylide electrophile to generate cathepsin X-selective activity-based probes. *ACS Chem. Biol.* 15: 718–727.

Nägler, D.K., Zhang, R., Tam, W., Sulea, T., Purisima, E.O., and Ménard, R. (1999). Human cathepsin X: a cysteine protease with unique carboxypeptidase activity. *Biochem*. 38: 12648–12654.

Obermajer, N., Svajger, U., Bogyo, M., Jeras, M., and Kos, J. (2008). Maturation of dendritic cells depends on proteolytic cleavage by cathepsin X. *J. Leukocyte Biol.* 84: 1306–1315.

Reinheckel, T. and Tholen, M. (2022). Low-level lysosomal membrane permeabilization for limited release and sublethal functions of cathepsin proteases in the cytosol and nucleus. *FEBS Open Bio*. 12: 694–707.

Schwenck, J., Maurer, A., Fehrenbacher, B., Mehling, R., Knopf, P., Mucha, N., Haupt, D., Fuchs, K., Greissinger, C.M., Bukala, D., et al. (2019). Cysteine-type cathepsins promote the effector phase of acute cutaneous delayed-type hypersensitivity reactions. *Theranostics* 9: 3903–3917.

Sereesongsaeng, N., Burrows, J.F., Scott, C.J., Brix, K., and Burden, R.E. (2023). Cathepsin V regulates cell cycle progression and histone stability in the nucleus of breast cancer cells. *Front. Pharmacol*. 14: 1271435.

Sevenich, L., Schurigt, U., Sachse, K., Gajda, M., Werner, F., Müller, S., Vasiljeva, O., Schwinde, A., Klemm, N., Deussing, J., et al. (2010). Synergistic antitumor effects of combined cathepsin B and cathepsin Z deficiencies on breast cancer progression and metastasis in mice. *Proc. Natl. Acad. Sci.* 107: 2497–2502.

Shirahama-Noda, K., Yamamoto, A., Sugihara, K., Hashimoto, N., Asano, M., Nishimura, M., and Hara-Nishimura, I. (2003). Biosynthetic processing of cathepsins and lysosomal degradation are abolished in asparaginyl endopeptidase-deficient mice. *J. Biol. Chem.* 278: 33194–33199.

Somoza, J.R., Zhan, H., Bowman, K.K., Yu, L., Mortara, K.D., Palmer, J.T., Clark, J.M., and McGrath, M.E. (2000). Crystal structure of human cathepsin V. *Biochem*. 39: 12543–12551.

Tamhane, T., Arampatzidou, M., Gerganova, V., Tacke, M., Illukkumbura, R., Dauth, S., Brix, K., Peters, C., and Reinheckel, T. (2014). The activity and localization patterns of cathepsins B and X in cells of the mouse gastrointestinal tract differ along its length. *Biol. Chem.* 395: 1201–1219.

Tamhane, T., Illukkumbura, R., Lu, S., Maelandsmo, G.M., Haugen, M.H., and Brix, K. (2016). Nuclear cathepsin L activity is required for cell cycle progression of colorectal carcinoma cells. *Biochimie*. 122: 208–218.

Turk, V., Stoka, V., Vasiljeva, O., Renko, M., Sun, T., Turk, B., and Turk, D. (2012). Review: cysteine cathepsins: from structure, function and regulation to new frontiers. *Biochim. Biophys. Acta - Proteins and Proteomics* 1824: 68–88.

Vasiljeva, O., Dolinar, M., Turk, V., and Turk, B. (2003). Recombinant human cathepsin H lacking the mini chain is an endopeptidase. *Biochem*. 42: 13522–13528.

Vasiljeva, O., Dolinar, M., Pungerčar, J.R., Turk, V., and Turk, B. (2005). Recombinant human procathepsin S is capable of autocatalytic processing at neutral pH in the presence of glycosaminoglycans. *FEBS Lett*. 579: 1285–1290.

Vasiljeva, O., Papazoglou, A., Kruger, A., Brodoefel, H., Korovin, M., Deussing, J., Augustin, N., Nielsen, B.S., Almholt, K., Bogyo, M., et al. (2006). Tumor cell-derived and macrophage-derived cathepsin B promotes progression and lung metastasis of mammary cancer. *Cancer Res.* 66: 5242–5250.

Verdoes, M., Oresic Bender, K., Segal, E., van der Linden, W.A., Syed, S., Withana, N.P., Sanman, L.E., and Bogyo, M. (2013). Improved quenched fluorescent probe for imaging of cysteine cathepsin activity. *J. Am. Chem. Soc.* 135: 14726–14730.

Wang, B., Shi, G.-P., Yao, P., Li, Z.Q., Chapman, H., and Bromme, D. (1998). Human cathepsin F. Molecular cloning, functional expression, tissue localization, and enzymatic characterization. *J. Biol. Chem.* 273: 32000–32008.

Wang, D., Kang, L., Chen, C., Guo, J., Du, L., Zhou, D., Li, G., Zhang, Y., Mi, X., Zhang, M., et al. (2022). Loss of legumain induces premature senescence and mediates aging-related renal fibrosis. *Aging Cell* 21: e13574.

Wilson, K.R., Liu, H., Healey, G., Vuong, V., Ishido, S., Herold, M.J., Villadangos, J.A., and Mintern, J.D. (2018). MARCH1-mediated ubiquitination of MHC II impacts the MHC I antigen presentation pathway. *PLoS One* 13: e0200540.

Yoon, M.C., Hook, V., and O'Donoghue, A.J. (2022). Cathepsin B dipeptidyl carboxypeptidase and endopeptidase activities demonstrated across a broad pH range. *Biochem*. 61: 1904–1914.

Yuan, F., Verhelst, S.H., Blum, G., Coussens, L.M., and Bogyo, M. (2006). A selective activity-based probe for the papain family cysteine protease dipeptidyl peptidase I/cathepsin C. *J. Am. Chem. Soc.* 128: 5616–5617.

Supplementary Material: This article contains supplementary material (https://doi.org/10.1515/hsz-2023-0355).